Supporting Information

A convenient and quantitative route to Sn(IV)-M [M = Ti(IV), Nb(V), Ta(V)] heterobimetallic precursors for dense mixed-metal oxide ceramics

Shashank Mishra,*[a] Erwann Jeanneau,[b] Stéphane Mangematin,[a] Henry Chermette,[c] Mahboubeh Poor Kalhor,[c] Guillaume Bonnefont,[d] Gilbert Fantozzi,[d] Sylvie Le Floch,[e] Stéphane Pailhes,[e] and Stéphane Daniele[a]

[a] Université Lyon 1, IRCELYON, CNRS-UMR 5256, 2 Avenue A. Einstein, 69626 Villeurbanne, France.

[b] Université Lyon 1, Centre de Diffractométrie Henri Longchambon, 5 rue de La Doua, 69100 Villeurbanne, France.

[c] Université Lyon1, Institut des Sciences Analytiques, CNRS UMR 5280, 43 boul. du 11 Nov. 1918, 69622 Villeurbanne, France.

[d] Université Lyon 1, INSA-Lyon, MATEIS CNRS-UMR 5510, 69621 Villeurbanne, France.

[e] Université Lyon 1, Institut Lumière Matière, CNRS-UMR 5306, 69622 Villeurbanne, France.

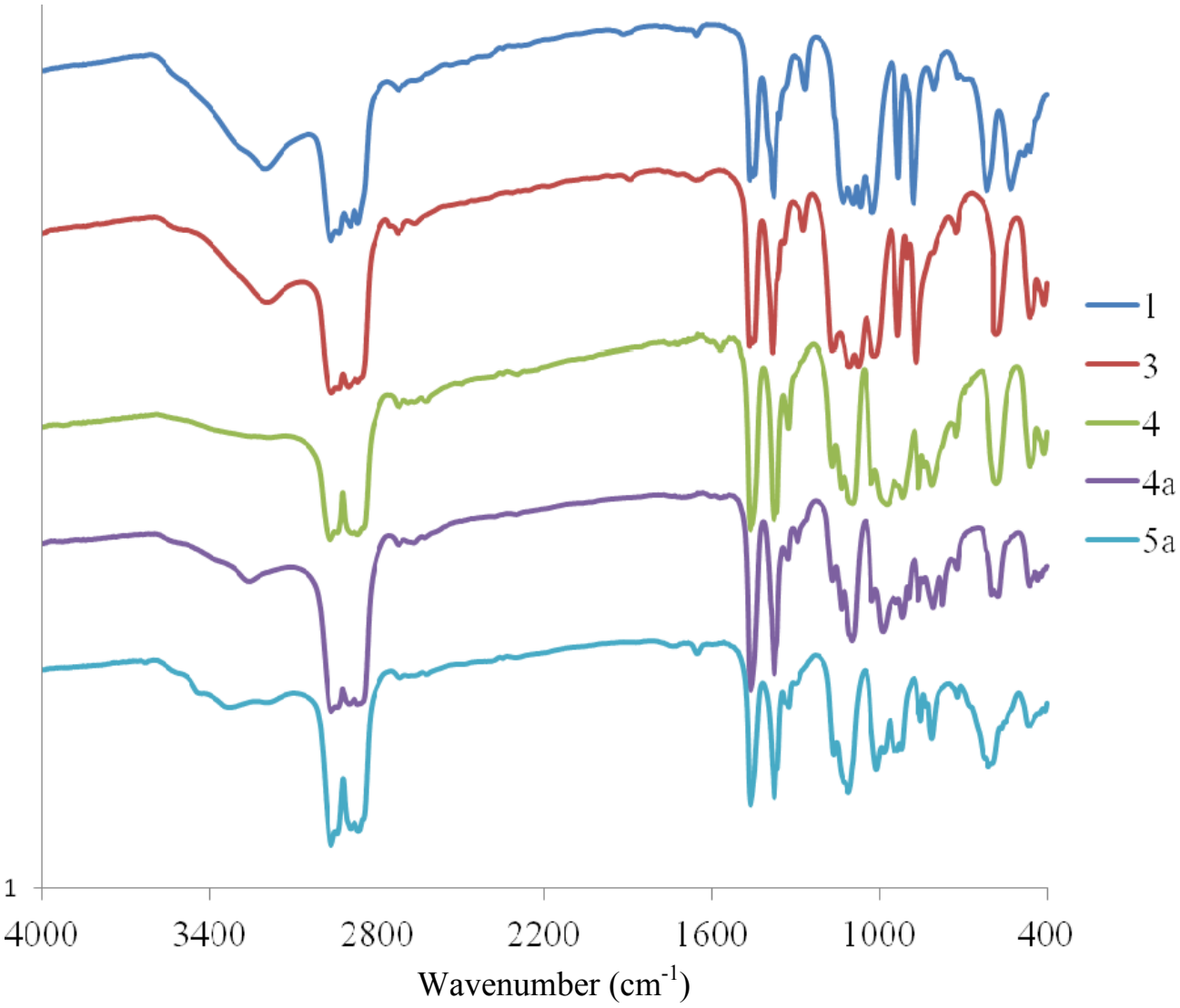

Figure S1. FT-IR spectra of **1-5** measured as nujol mulls.

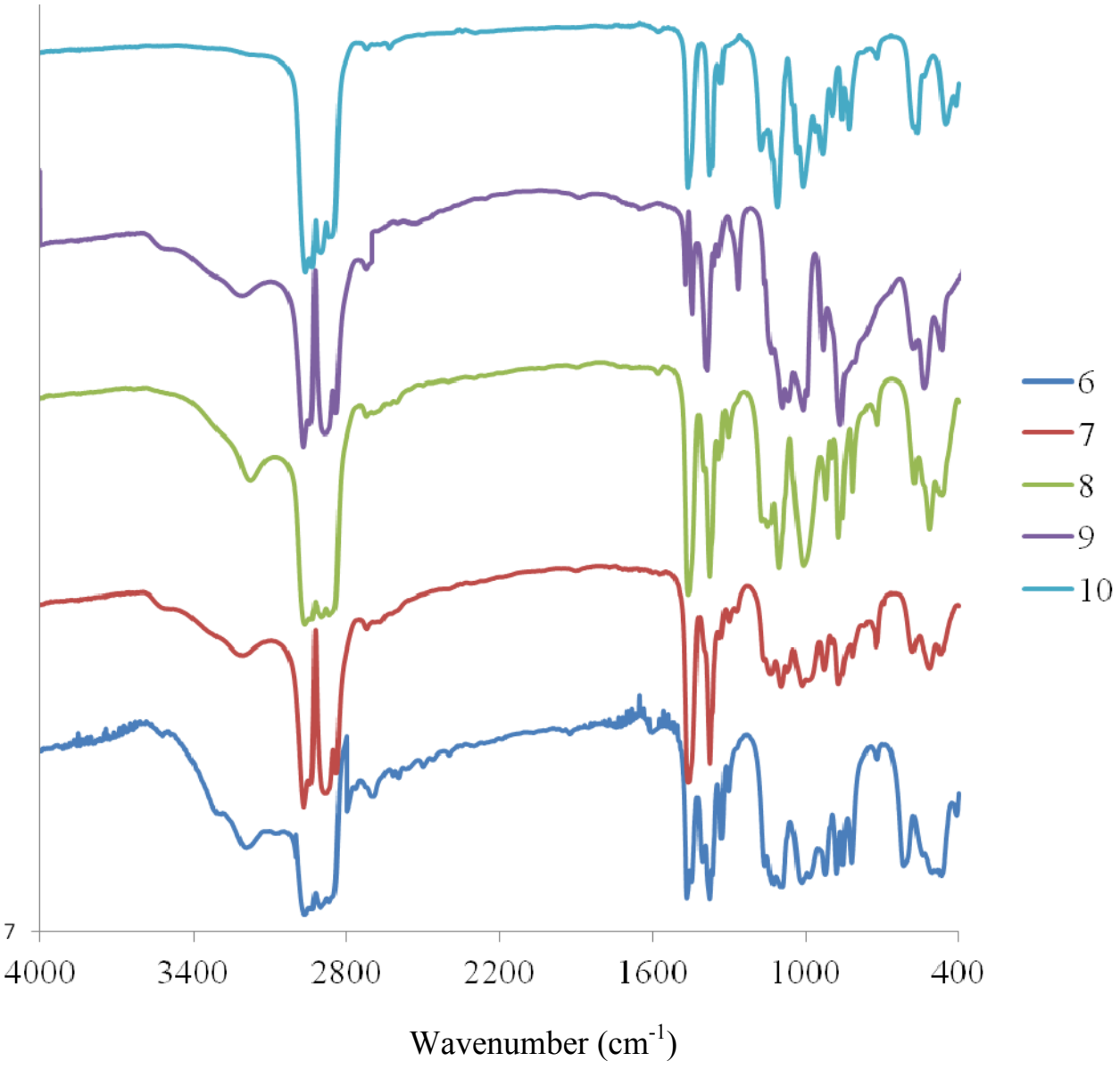

Figure S2. FT-IR spectra of **6-10** measured as nujol mulls.

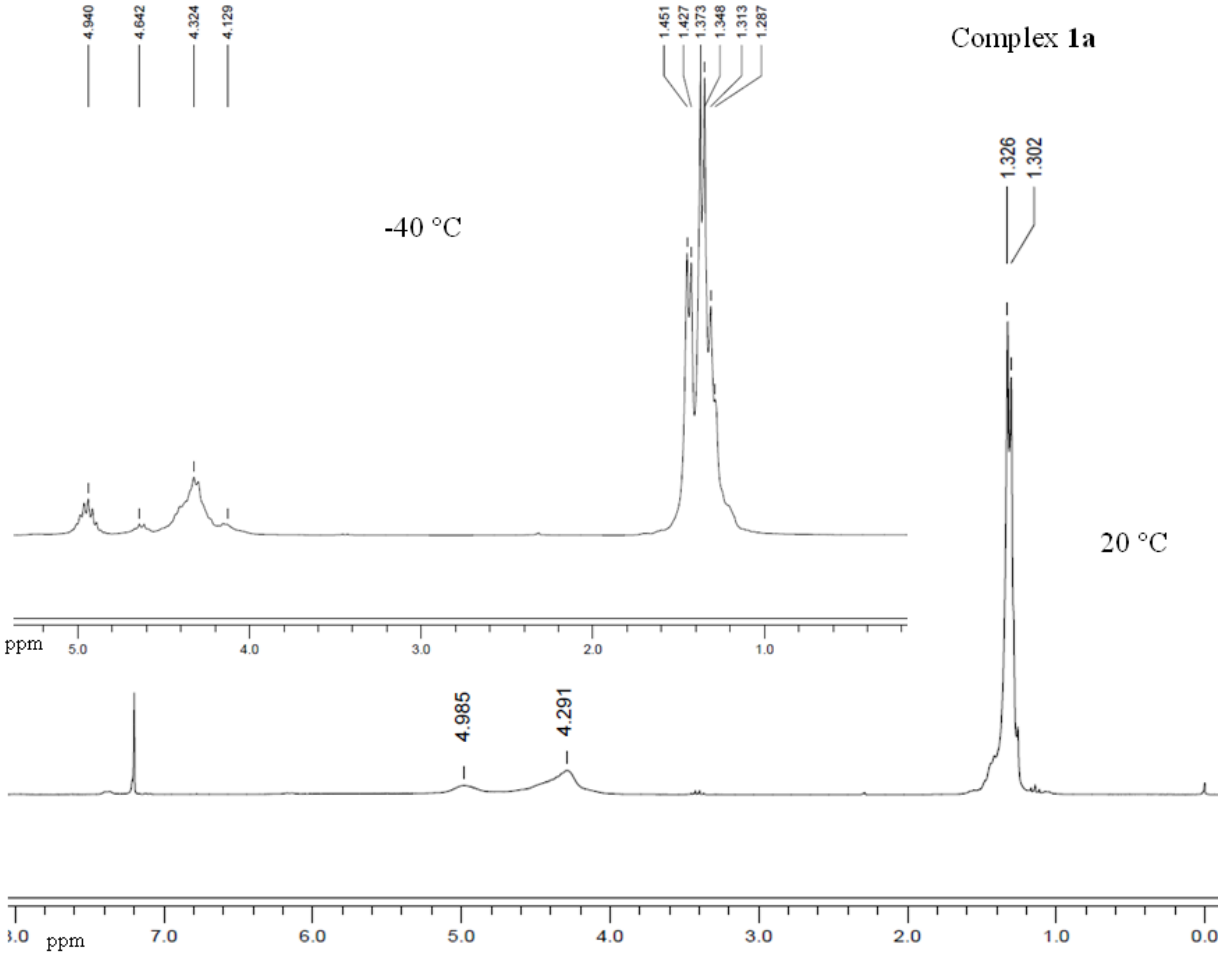

Figure S3. Variable temperature ^{1}H NMR spectra of **1a** in $CDCl_3$.

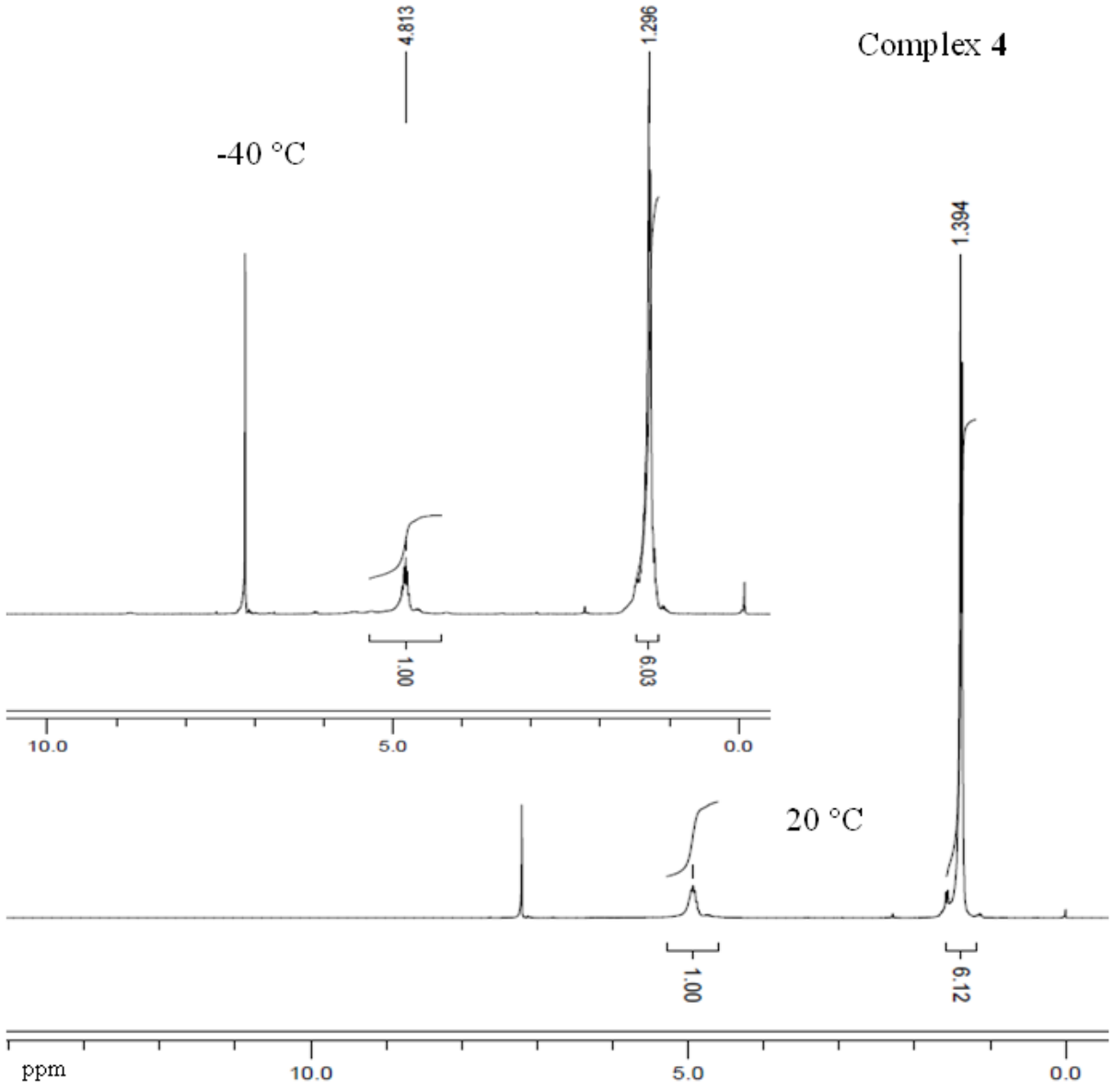

Figure S4. Variable temperature ^{1}H NMR spectra of **4** in $CDCl_3$.

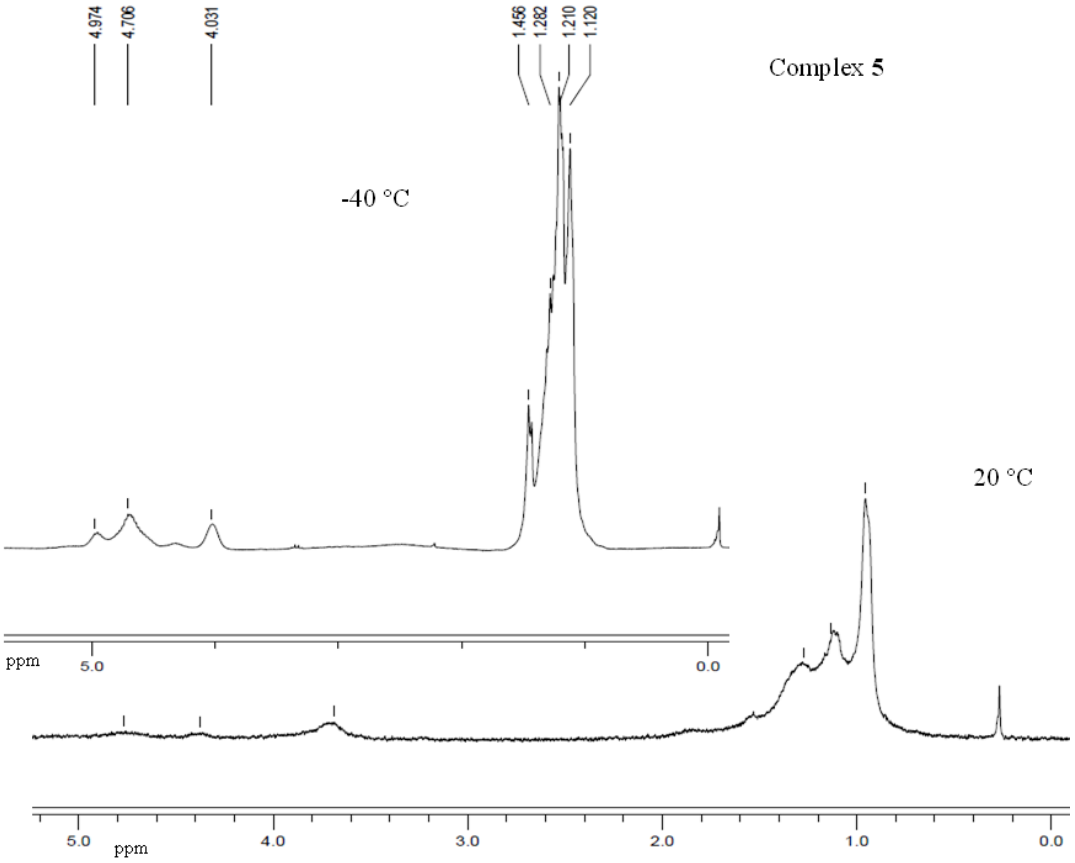

Figure S5. Variable temperature ^{1}H NMR spectra of **5** in $CDCl_3$.

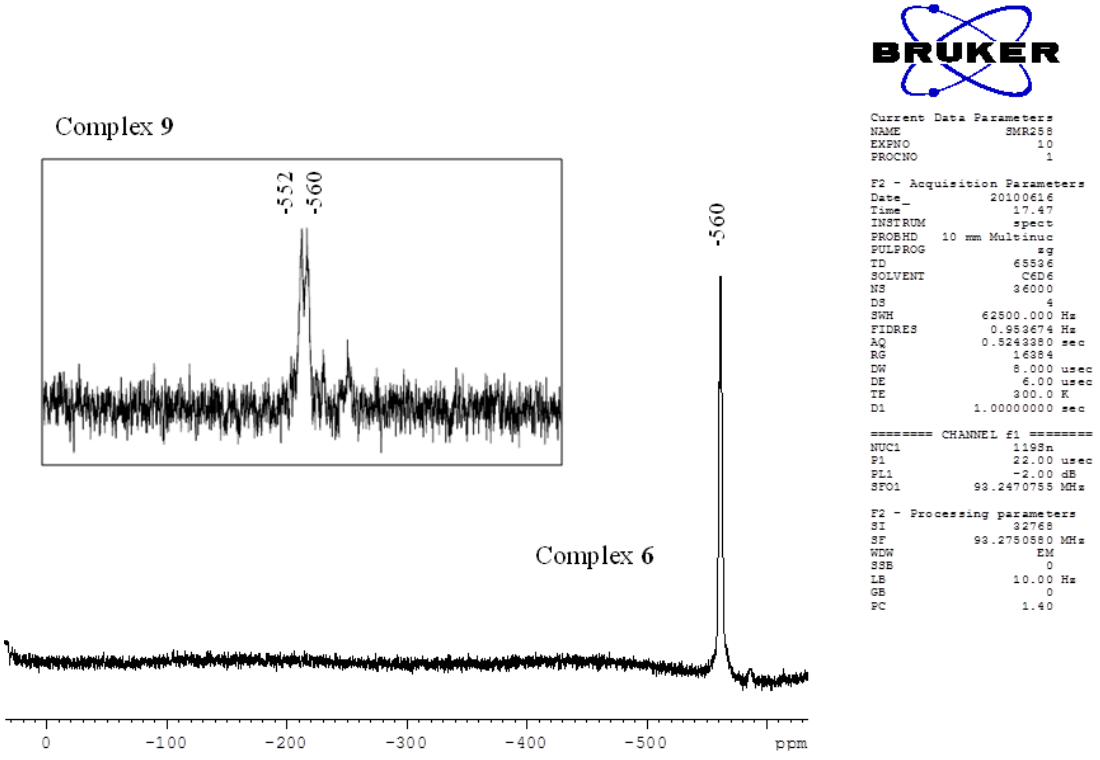

Figure S6. ^{119}Sn NMR spectra of **6** and **9** (inset) measured in toluene.

X-Ray Structures

Depending on crystallization conditions, the complex $[SnCl_4(\mu\text{-}OEt)_2Ti(OEt)_2(HOEt)_2]$ **1** was isolated without or with a solvated ethanol molecule. In the crystal structure of the unsolvated form **1a,** which contains two independent molecules in the unit cell, the two adducting EtOH molecules on titanium metal center are in a *trans* position [O3–Ti1–O6 = 168.8(4)°], forming two intramolecular H-bonding with neighboring chloride ligands present on tin metal center [H3···Cl1 = 2.388(3) Å; O6···Cl4 = 2.267(3) Å] (Fig. S7). In contrast, the solvated form of the crystal structure (**1b**) contains these two EtOH molecules in a *cis* position [O3–Ti–O4 = 79.7(1)°],[14] which are involved in intra- and intermolecular H-bonding with chloride anion present on tin center [H3···Cl3 = 2.385(3) Å] and the solvated ethanol molecule [H4···O7 = 1.747(3) Å], respectively, the later also being involved in additional intermolecular H-bonding with chloride atom of another molecule [H7···Cl4 = 2.314(3) Å] (Fig. S8). This difference in intra- and intermolecular H-bonding leads to two different molecular packing for the **1a** and **1b**. Additional intermolecular short interactions also exists between hydrogen atoms of ethoxy groups and chloride ligand (H···Cl = 2.901-2.920 Å). Except for the difference in relative position of the two adducting EtOH molecules on Ti center, the molecular structures of two forms **1a** and **1b** are very similar at dinuclear level, which can be described as two distorted octahedra TiO_6 and $SnCl_4O_2$ combined through a common edge comprising of two oxygen atoms O1 and O2. As expected, the average bridging Ti–O (OEt) distance is longer (2.048 Å) than the terminal Ti–O (OEt) one (1.793 Å) but almost similar to that involving adducting EtOH ligand (2.057 Å), a trend that is observed in the other Ti heterometal alkoxides also reported in this article. The two chloride ligands on Sn(IV) center involved in intramolecular H-bonding form significantly longer Sn-Cl bonds [at Sn1-Cl1 2.439(4) and Sn1-Cl4 2.460(4) Å] than the remaining two Sn-Cl bonds [Sn1-Cl2 2.364(4) and Sn1-Cl3 2.352(4) Å]. The av. non-bonded Sn···Ti distance in **1a** and **1b** is 3.335 Å. The

terminal O4–Ti–O5 bond angle at 101.9(6) ° is significantly greater than the angle of 71.4(3)° subtended by the O–Ti–O bonds involved in bridging.

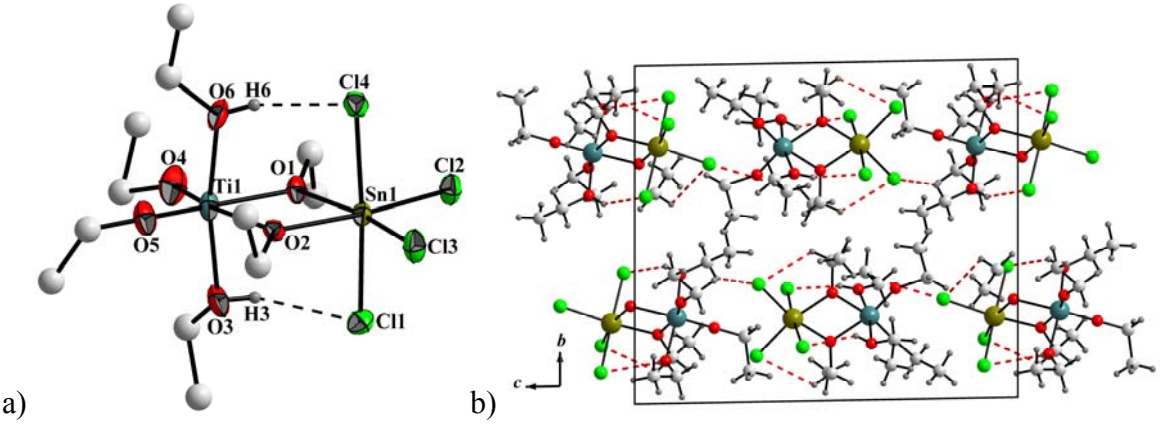

a) b)

Figure S7. (a) Perspective views of **1a** with displacement ellipsoids drawn at the 30% probability level. Carbon atoms are drawn as ball and stick and the H-atoms on alkyl groups are omitted for clarity. (b) Molecular packing of **1a** showing intra- and inter-molecular H-bondings. Selected bond lengths (Å) and angles (°): Ti1–O1 2.048(10), Ti1–O3 2.078(12), Ti1–O5 1.739(11), Sn1–O1 2.055(8), Sn1–Cl1 2.439(4), Sn1–Cl2 2.364(4), O1–Ti1–O2 71.4(3), O4–Ti1–O5 101.9(6), O3–Ti1–O6 168.8(4), O6–Ti1–O4 93.2(6), O1–Sn1–O2 71.1(3), Cl2–Sn1–Cl3 98.58(14), Cl4–Sn1–Cl2 90.80(15).

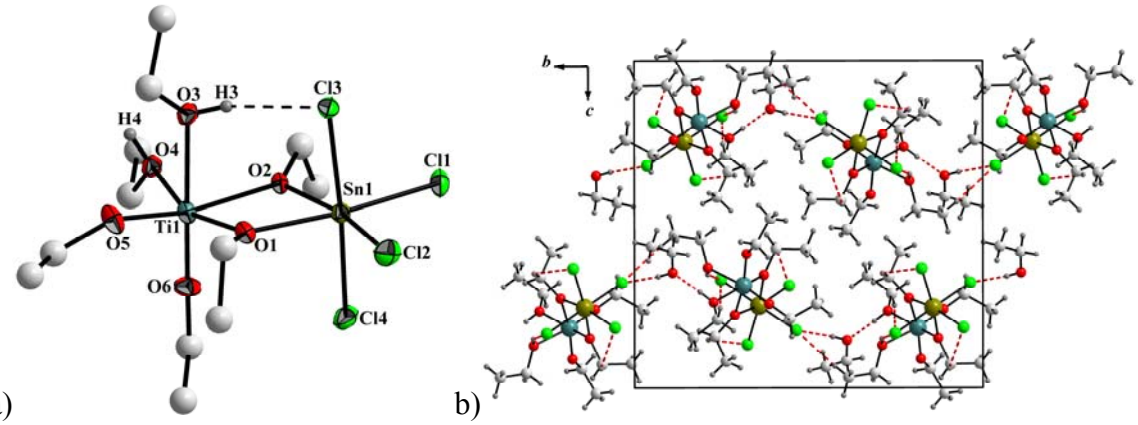

a) b)

Figure S8. (a) Perspective views of **1b** with displacement ellipsoids drawn at the 30% probability level. The solvated ethanol molecule and H-atoms on alkyl groups are omitted for clarity. (b) Molecular packing of **1b** showing intra- and inter-molecular H-bondings. Selected bond lengths (Å) and angles (°): Ti1–O1 1.995(3), Ti1–O3 2.177(3), Ti1–O4 2.053(3), Ti1–O5 1.768(4), Sn1–O1 2.093(3), Sn1–Cl1 2.3696(13), Sn1–Cl3 2.4385(12), Sn1–Cl4 2.4263(13), O2–Ti1–O1 73.22(13), O3–Ti1–O4 79.73(13), O4–Ti1–O5 97.84(18), O5–Ti1–O6 99.37(19), O1–Sn1–O2 71.43(12), Cl3–Sn1–Cl1 91.64(5), Cl2–Sn1–Cl1 96.89(6).

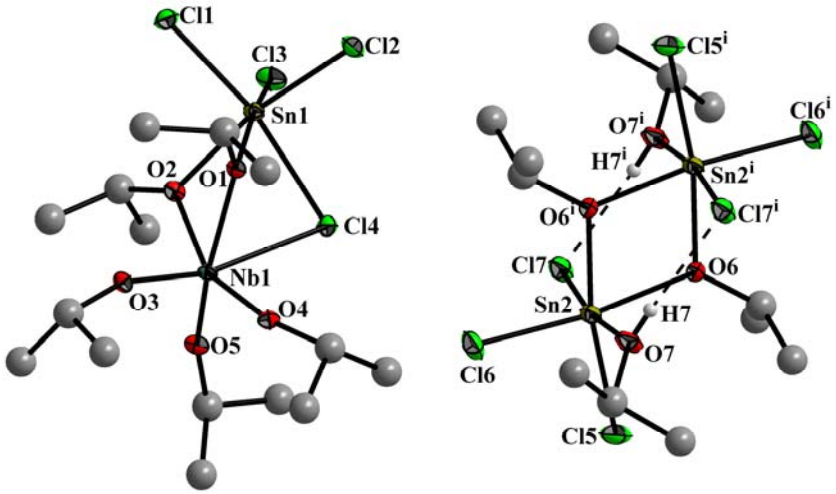

Figure S9. Perspective views of $[SnCl_3(\mu\text{-}Cl)(\mu\text{-}OPr^i)_2Nb(OPr^i)_3][Sn_2Cl_6(\mu\text{-}OPr^i)_2(Pr^iOH)_2]$ (**4a**) with displacement ellipsoids drawn at the 30% probability level. Carbon atoms are drawn as ball and stick and H-atoms are omitted for clarity. Selected bond lengths (Å) and angles (°): Sn1–O12.095(3), Nb1–O12.131(3) Sn1–O2 2.115(3), Nb1–O2 2.116(3), Nb1–O31.814(3), Sn2–O6 2.096(3), Sn2–O7 2.164(3), Sn1–Cl4 2.527(1), Sn1–Cl1 2.370(1), Sn1–Cl2 2.364(1), Nb1–Cl4 2.714(1), Sn2–Cl7 2.400(1), O2–Sn1–Cl4 76.63(8), Cl1–Sn1–Cl2 96.29(4), Cl6–Sn2–Cl5 91.98(5), O1–Nb1–O2 70.94(10), O4–Nb1–O3 100.25(13), O1–Nb1–Cl4 71.87(7), $O6^i$–Sn2–O6 72.57(12). Symmetry codes: (i) $-x+1, -y+2, -z+2$.

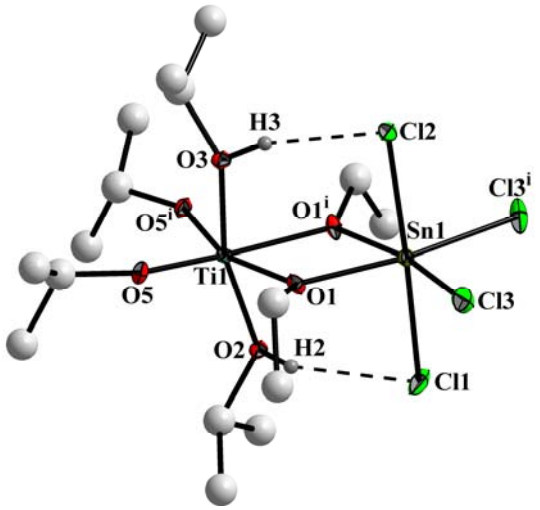

Figure S10. Perspective views of **6** with displacement ellipsoids drawn at the 30% probability level. C-atoms are drawn as ball and stick and the solvated ethanol molecule and H-atoms on alkyl groups are omitted for clarity. Selected bond lengths (Å) and angles (°): Ti1–O1 2.072 (2), Ti1–O2 2.073 (4), Ti1–O3 2.068(4), Ti1–O5 1.800(9), Sn1–O1 2.080(2), Sn1–Cl1 2.439(1), Cl2···H3 2.315(1), $O1^i$–Ti1–O1 71.6(1), O1–Sn1–$O1^i$ 71.3(1), Cl3–Sn1–$Cl3^i$ 97.56(5), Cl1–Sn1–Cl2 177.50(5). Symmetry code (i): x, ½-y, z.

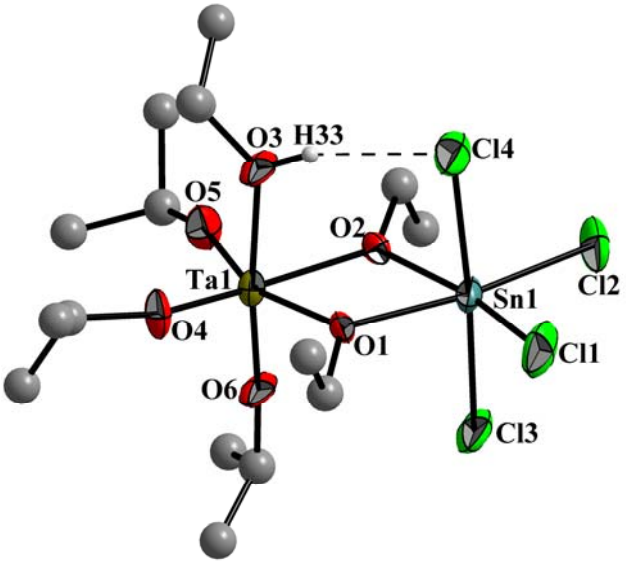

Figure S11. Perspective views of **8** with displacement ellipsoids drawn at the 30% probability level. Carbon atoms are drawn as ball and stick and H-atoms of alkyl groups are omitted for clarity. Selected bond lengths (Å) and angles (°): Ta1–O1 2.095(8), Ta1–O3 2.117(8), Ta1–O6 1.783(8), Sn1–O1 2.107(7), Sn1–Cl1 2.349(5), Sn1–Cl4 2.431(4), Ta1···Sn1 3.432(1), O2–Ta1–O1 70.6(3), O5–Ta1–O3 86.5(5), O5–Ta1–O4 102.4(4), O6–Ta1–O4 96.4(5), O2–Sn1–O1 69.9(3), Cl2–Sn1–Cl1 97.77(19), Cl4–Sn1–Cl2 90.27(18).

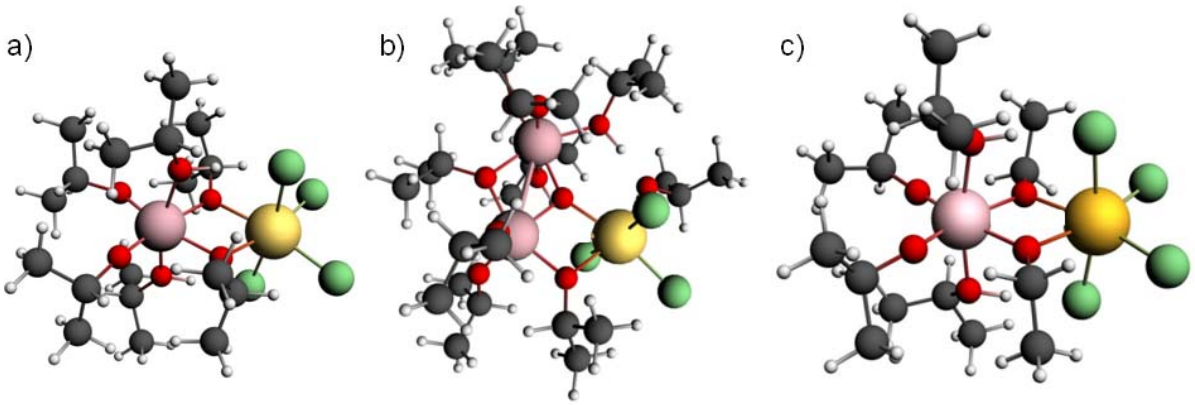

Figure S12. DFT-optimized structures of $SnCl_3(\mu\text{-}Cl)(\mu\text{-}OPr^i)_2Nb(OPr^i)_3$] **4** (a), [$SnCl_3(\mu_3\text{-}O)(\mu\text{-}OPr^i)_2Ti_2(OPr^i)_5(HOPr^i)_2$] **5** (b), and [$SnCl_4(\mu\text{-}OEt)_2Ti(Pr^iO)_2(Pr^iOH)_2$] **6** (c). Color scheme: Sn (yellow), Nb/Ti (light pink), Cl (green), O (red), C (dark grey), H (white).

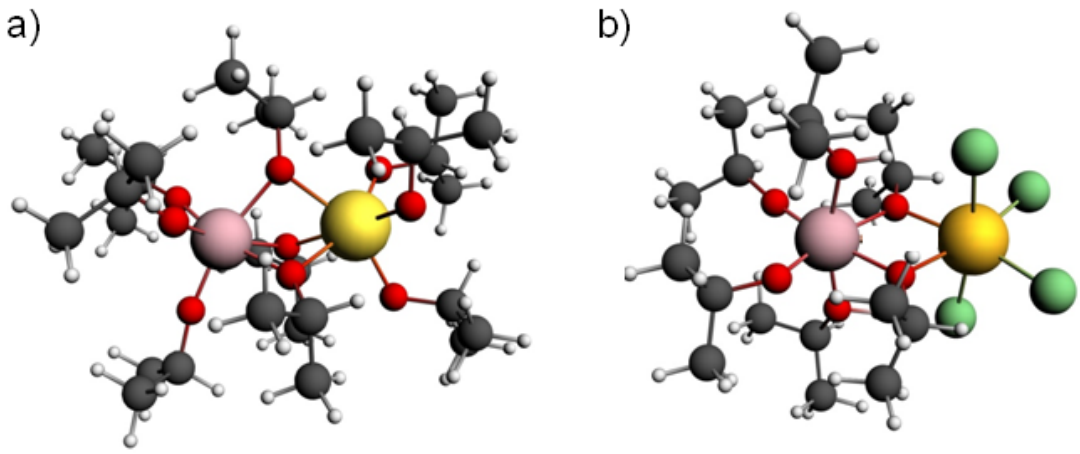

Figure S13. DFT-optimized structures of model compounds **4_mod** and **6_mod**. Color scheme: Sn (yellow), Nb/Ti (light pink), Cl (green), O (red), C (dark grey), H (white).

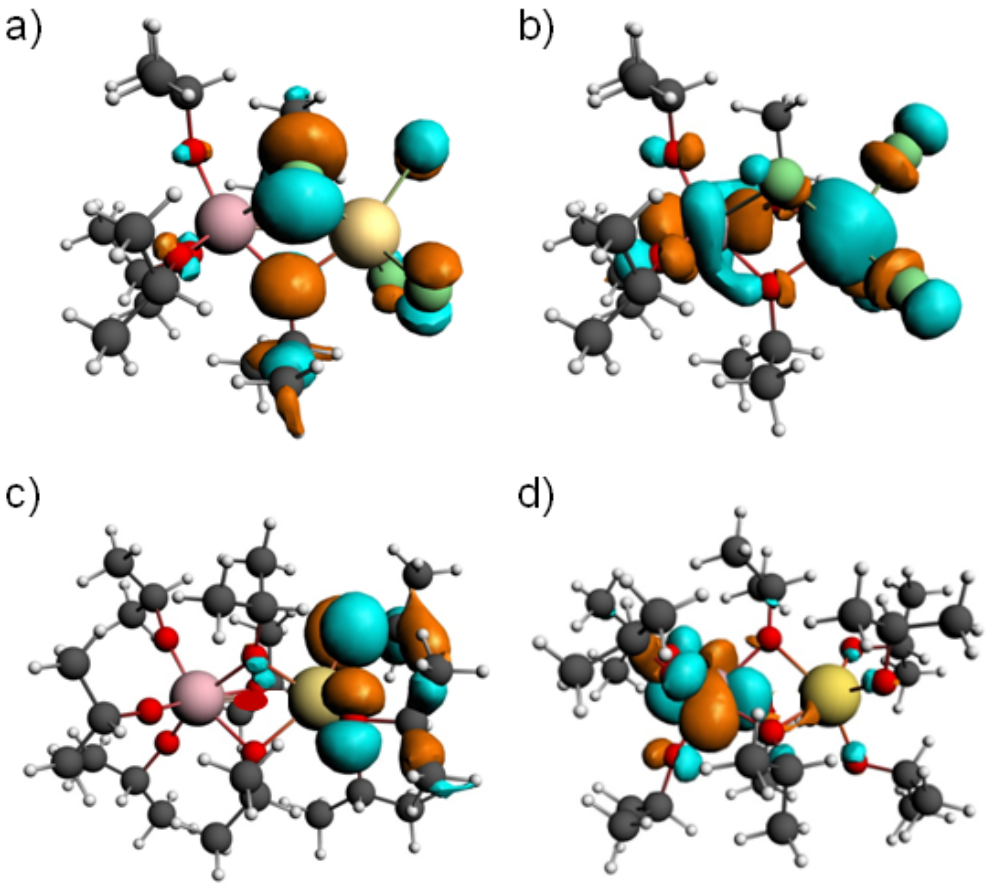

Figure S14. DFT-optimized structures with HOMO and LUMO of **4** (a & b) and **4_mod** (c & d). Color scheme same as that described in Figures S12 and S13.

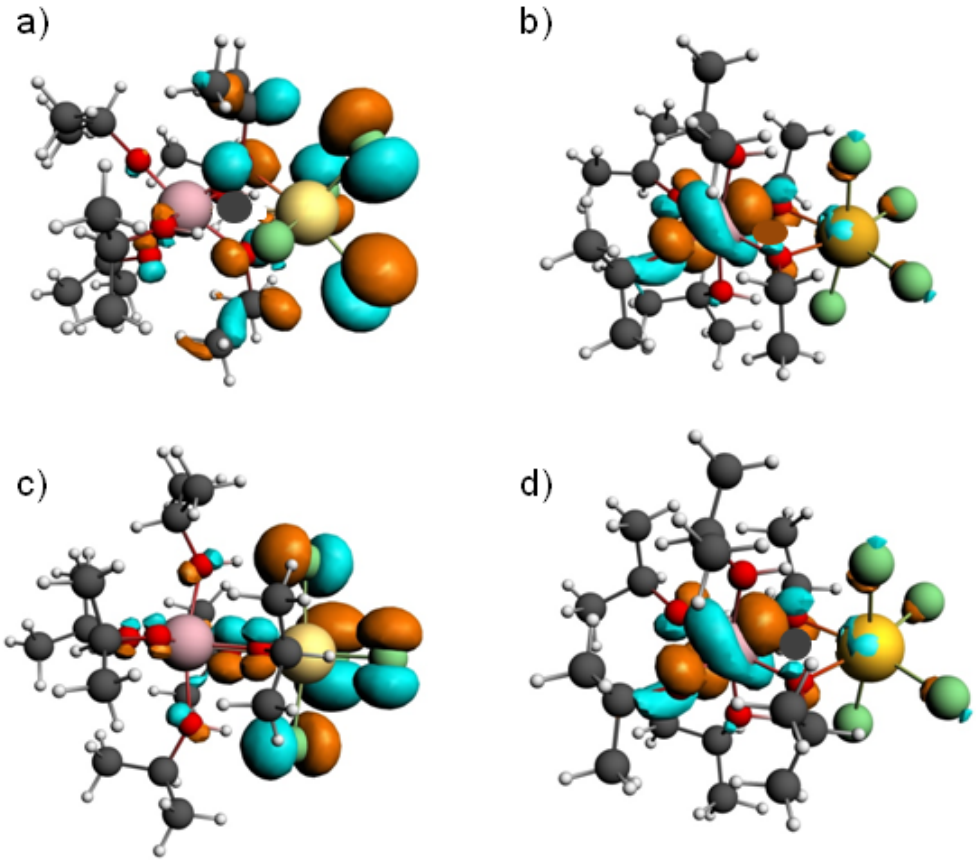

Figure S15. DFT-optimized structures with HOMO and LUMO of **6** (a & b) and **6_mod** (c & d). Color scheme same as that described in Figures S12 and S13.

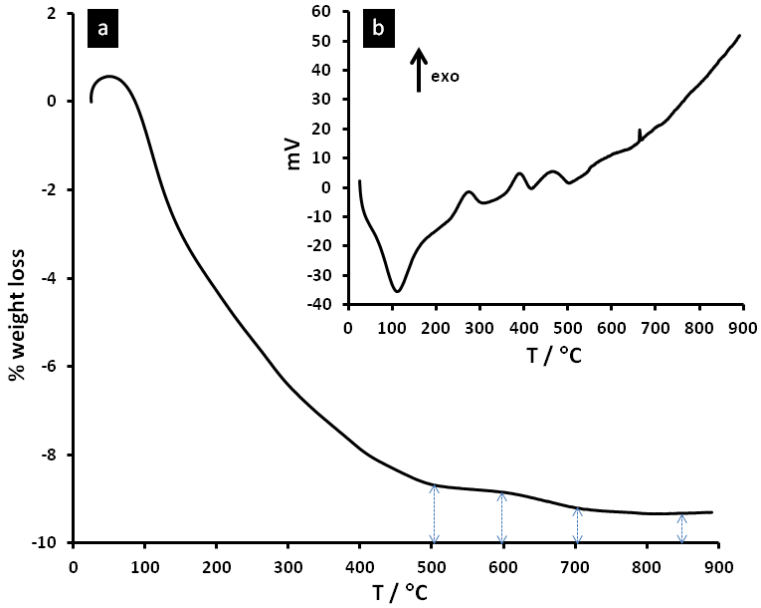

Figure S16. TGA (a) and DTA (b) curves of the as-prepared powder obtained from the hydrolysis of the precursor **1**.

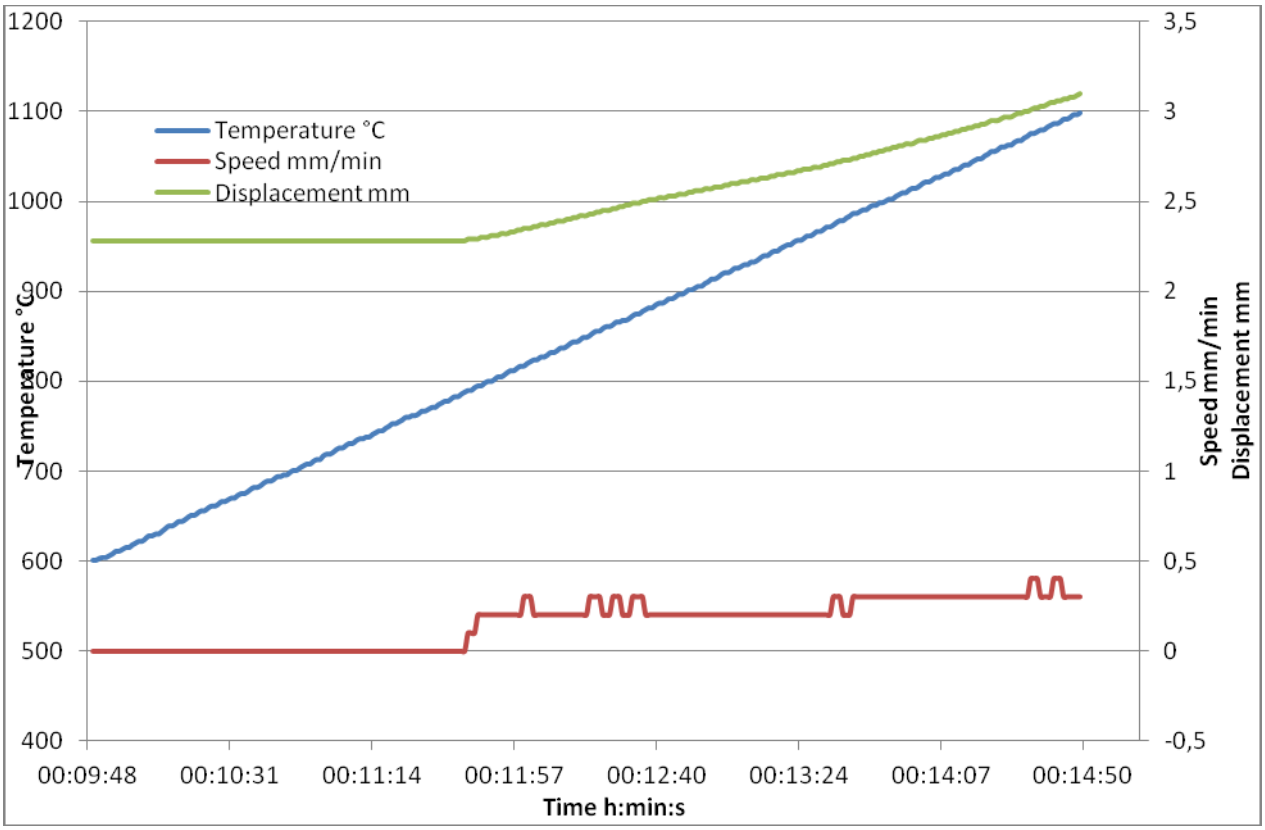

Figure S17: Sintering cycle of $Sn_{0.5}Ti_{0.5}O_2$ NPs calcined at 500°C/ 4h.

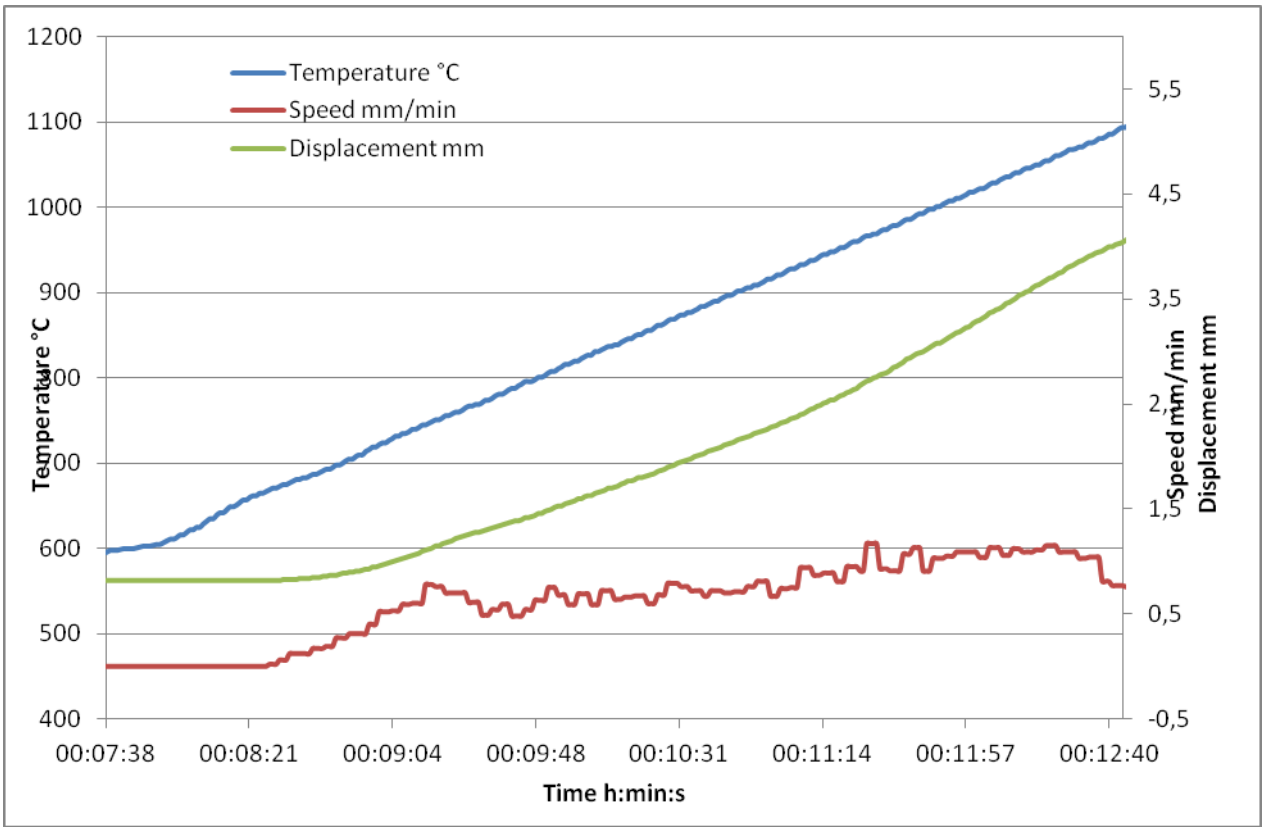

Figure S18: Sintering cycle of $Sn_{0.5}Ti_{0.5}O_2$ NPs calcined at 600°C/ 4h.

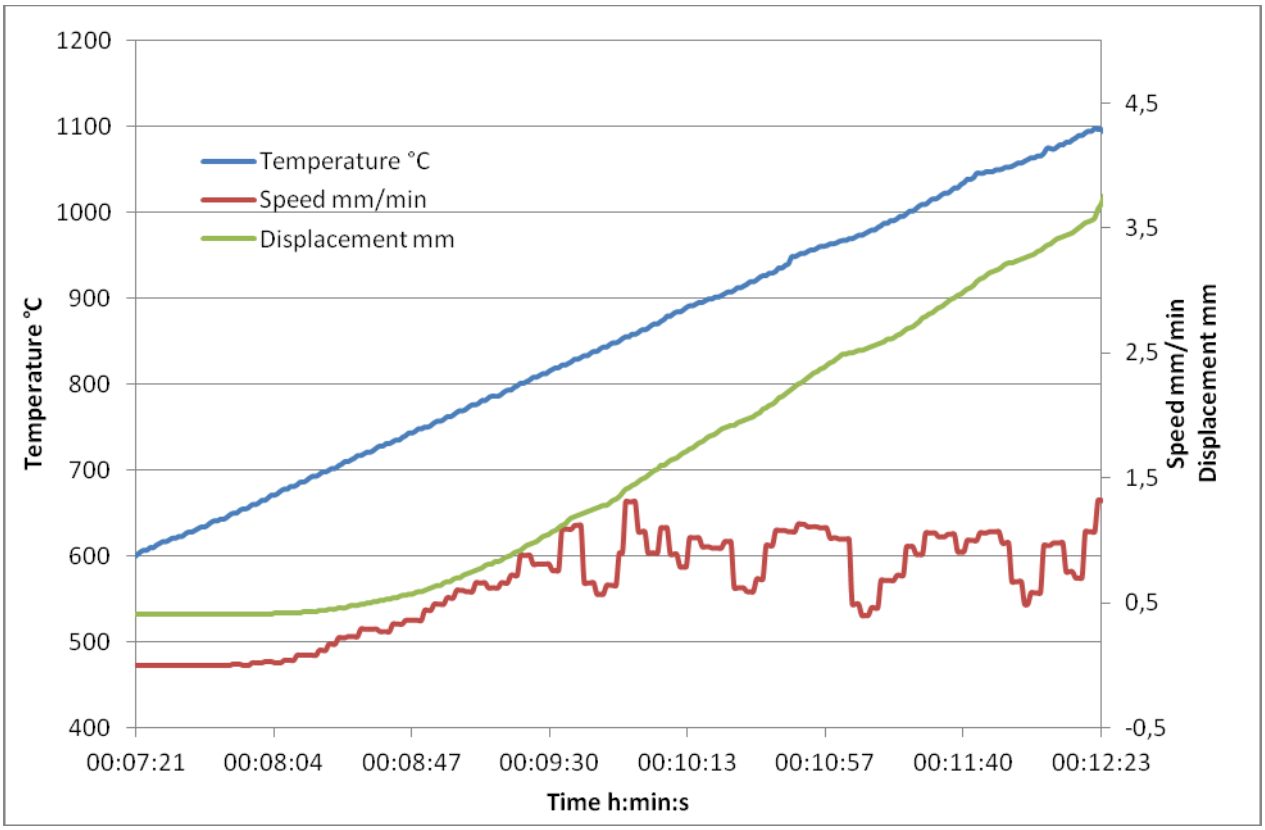

Figure S19: Sintering cycle of $Sn_{0.5}Ti_{0.5}O_2$ NPs calcined at 700°C/ 4h

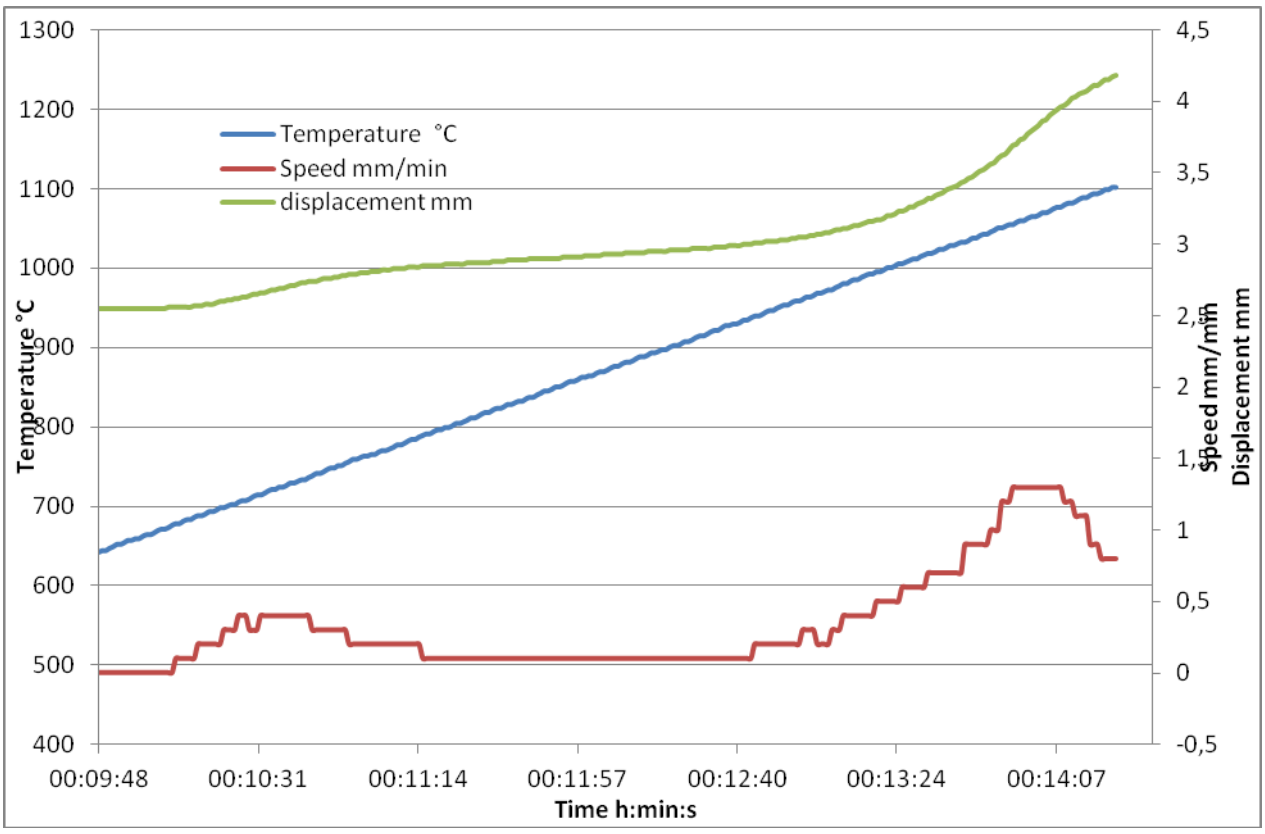

Figure S20: Sintering cycle of $Sn_{0.5}Ti_{0.5}O_2$ NPs calcined at 850°C/ 2h.

Table S1. HOMO-LUMO gap and some selected bond lengths (Å) in the DFT-optimized structures of **4-6**, **4_mod** and **6_mod**.

Compound	LUMO (eV)	HOMO (eV)	gap-hardness (eV)	Selected av. bond lengths (Å)
4	-3.296	-6.276	2.98	Sn–μ-OR = 2.21; Nb–μ-OR = 2.12; Nb–$OR_{terminal}$ = 1.90; Sn–μ-Cl = 2.66; Nb–μ-Cl = 2.71; Sn–$Cl_{terminal}$ =2.40, 2.40, 2.42*; Sn···Nb = 3.34. *trans to μ-Cl
4_mod	-2.470	-5.008	2.53	Sn–μ-OR = 2.24; Sn–$OR_{terminal}$ = 2.45, 2.46; Nb–μ-OR = 2.14; Nb–$OR_{terminal}$ = 1.91; Sn···Nb = 3.23.
5	-2.881	-5.617	2.73	Sn–μ-OR = 2.20; Sn–$OR_{terminal}$ = 2.08; Ti–μ-OR = 1.94, 2.03; Ti–$OR_{terminal}$ = 1.83; Ti–$OHR_{terminal}$ = 2.12, 2.26;Sn-$Cl_{terminal}$ =2.44, 2.45, 2.57; Sn···Ti = 3.32, 3.94; Ti···Ti = 3.18.
6	-3.102	-6.152	3.04	Sn–μ-OR = 2.20; Ti–μ-OR = 2.05; Ti–$OR_{terminal}$ = 1.81; Ti–$OHR_{terminal}$ = 2.15; Sn–$Cl_{terminal}$ = 2.41, 2.53*; Sn···Ti = 3.46. * H-bond
6_mod	-3.175	-6.046	2.85	Sn–μ-OR = 2.19; Ti–μ-OR = 2.05; Ti–$OR_{terminal}$ = 1.82; Ti–$OHR_{terminal}$ = 2.15; Sn–$Cl_{terminal}$ = 2.41, 2.54*; Sn···Ti = 3.47. * H-bond